Inorg. Chem. **2008**, *47*, 11351−11360

Synthesis, Characterization, and Sorption Properties of Amorphous Titanium Phosphate and Silica-Modified Titanium Phosphates

Marina V. Maslova,[†] Daniela Rusanova,[*,‡] Valeri Naydenov,[§] Oleg N. Antzutkin,[‡] and Lidia G. Gerasimova[†]

Tananaev Institute of Chemistry and Technology of Rare Elements and Mineral Raw Materials, Kola Science Center, Russian Academy of Sciences, Fersman st. 26a, Apatity, Murmansk region, 184209 Russia, Division of Chemistry, Luleå University of Technology, 97187 Luleå, Sweden, and SunPine AB, Box 76, 941 22 Piteå, Sweden

Received July 8, 2008

Amorphous titanium hydroxyphosphate with formula $Ti(OH)_{1.36}(HPO_4)_{1.32} \cdot 2.3H_2O$ and a new silica-modified titanium hydroxyphosphate with a general formula $Ti(OH)_{2x}(HPO_4)_{2-x} \cdot ySiO_2 \cdot nH_2O$ are synthesized and characterized using IR, TG, XRD, SEM, solid-state NMR, and BET techniques. It is concluded that SiO_2 is evenly distributed within the titanium phosphate (TiP) agglomerates and that neither the separate silica phase nor the titanium silicates are formed during the synthesis of silica-modified titanium hydroxyphosphate. Correlations between the texture, ion-exchange properties of the amorphous titanium hydroxyphosphate, and the amount of SiO_2 present within the TiP matrix are established. Sorption properties of silica-modified titanium hydroxyphosphate toward Cs^+ and Sr^{2+} are studied in a series of samples with an increasing amount of silica, at different pH, and in NaCl solutions with a varying ionic strength. It is found that sorption of Cs^+ does not depend practically on the amount of SiO_2 present, whereas the Sr^{2+} uptake drastically decreases with an increase of silica amount. The effects of pH and of the electrolyte concentration on the sorption behavior of titanium phosphate are discussed in terms of ionic hydration shell and titanium phosphate structural specificity. The kinetics of sorption processes is also investigated, and the diffusion coefficients for cesium and strontium are obtained.

Introduction

Synthetic inorganic ion exchangers have received much attention in the last decades. Among these materials, titanium phosphates (TiP) are given a special attention.[1−7] Their high selectivity to metal cations is promising in the fabrication of new materials for industrial and nuclear waste treatments, recovery of toxic elements, syntheses of high-pure grade reagents, and in various chromatographic separations.[8−12] The desired properties of such materials can be tailored by careful selection of the synthesis conditions. Thus, materials with excellent thermal and radiation stability, enhanced selectivity toward heavy metal ions, and high resistance to oxidation can be prepared.

It has been reported that amorphous and crystalline TiP are produced with different P/Ti ratios depending on the starting conditions.[13] The amorphous form is obtained when the complex cationic species initially present in the synthesis solution polymerize to form agglomerates with variable

* To whom correspondence should be addressed. E-mail: Daniela.Rusanova@ltu.se.
† Russian Academy of Sciences.
‡ Luleå University of Technology.
§ SunPine AB.

(1) Clearfield, A.; Stynes, J. A. *J. Inorg. Nucl. Chem.* **1964**, *26*, 117.
(2) Alberti, G.; Torracca, E. *J. Inorg. Nucl. Chem.* **1968**, *30*, 317.
(3) Bhaumik, A.; Inagaki, S. *J. Am. Chem. Soc.* **2001**, *123*, 691.
(4) Nilchi, A.; Maragheh, M. G.; Khanchi, A. *J. Inorg. Nucl. Chem.* **2004**, *261*, 393.
(5) Szirtes, L.; Riess, L.; Megyeri, J. *Central European J Chem.* **2007**, *5*, 516.
(6) Bruque, S.; Aranda, M. A. G.; Losilla, E. R. *Inorg. Chem.* **1995**, *34*, 893.
(7) Bortun, A. I.; Bortun, L.; Cleafield, A. *J. Mater. Res.* **1996**, *11*, 2490.
(8) Solbra, S.; Allison, N.; Waite, S. *Environ. Sci. Technol.* **2001**, *35*, 626.
(9) Trobajo, C.; Llavona, R.; Podriguez, J. *Mater. Res. Bull.* **1989**, *24*, 1453.
(10) Bortun, A. I.; Bortun, L.; Poojary, D. M. *Chem. Mater.* **2000**, *12*, 294.
(11) De Oliveira, S. F.; Airoldi, C. *Microchim. Acta* **1993**, *110*, 95.
(12) Cardoso, V. A.; Souza, A. G.; Sartoratto, P. P. C.; Nunes, L. M. *J. Colloid Surf., A* **2004**, *248*, 145.
(13) Schmutz, C.; Barboux, P.; Ribot, F. *J. Non-Cryst. Solids* **1994**, *170*, 250.

10.1021/ic801274z CCC: $40.75
Published on Web 10/29/2008

properties. The crystalline TiP on the other hand is formed during refluxing of a gel-like mixture of amorphous titanium phosphate and phosphoric acid. The formation mechanism involves dissolution followed by nucleation and crystal growth.[14]

The crystalline TiP materials have well-defined structures which make them dedicated ion exchangers, that is, selective toward specific cations. In contrast, the amorphous titanium phosphates possess ill-defined layered type structures with van der Waals forces holding the layers together. These structural differences may provide a greater possibility for the amorphous TiP′s to act as ion exchangers, for example toward wide range of cations with dissimilar sizes and charges. Thus, these materials are expected to show different accessibility due to distributions of active sites with different local environments rather than the discrete attainability achieved through well-defined pathways. It has been found that titanium and zirconium phosphates with low crystallinity show a relatively high affinity to some di- and trivalent cations, individually present in solution or in a mixture.[15−17] The ion-exchange behavior of these materials is governed by the structural specificity of TiP whether layer- or framework-type structures are obtained at different synthesis conditions. The amorphous titanium phosphates can be modified through a reaction with alkyl amines that leads to formation of amine intercalates. Thus, obtained intercalates are characterized with larger layer spacing, *d*, rather than with the initial materials. This broadening of *d* points out the materials' layer structure.[7]

One of the main drawbacks that hinder the introduction of TiP′s on industrial scale applications for example exchange-column operations is the fact that they are often produced as fine powders. The synthesized powders are typically processed further into larger agglomerates having various shapes such as beads, pellets, monoliths, and so forth, which are tailored to the particular application. Granulated TiP's materials are produced either by sol−gel technology or extrusion molding.[18] According to the first method, $TiCl_4$ and phosphoric acid are mixed together and then added dropwise into a column filled with an organic solvent. Spherical granules of titanium hydrogel are then obtained which convert into a xerogel upon drying. The extrusion molding approach is generally preferred for synthesizing amorphous compounds. Authors have developed a combined method that involves obtaining the amorphous titanium phosphates with subsequent mechanical granulation of the final product.[19] In a typical procedure, a silicate solution is added into the synthesis solution and acts as a binder for the synthesized amorphous TiP particles. In this manner, the granules are provided with mechanical strength that is needed during transportation, loading, stress under operating conditions, and so forth.

This work reports on syntheses, characterization, and sorption properties of granulated and powder Ti(IV) hydroxyphosphate (TiP) and its silica-modified analogues (TiPSi). One aspect in which this article contributes to the existing reports on TiP syntheses is the use of titanyl sulfate as a source for titanium in comparison to published synthesis protocols where titanium chloride source dominates. The use of titanyl sulfate on one hand eliminates the environmental concerns associated with the use of titanium chloride source in a case of large scale synthesis. On the other hand, the titanium sulfuric acid solutions are characterized with presence of different Ti(IV) species due to hydrolysis and polymerization processes that take place. These species are expected to play a major role in formation and properties of final titanium phosphates. Another aspect of this article is to develop a preparation protocol which utilizes a soft hydrothermal synthesis rather than reflux conditions or autogenous conditions typical for autoclaves syntheses. A contribution to the knowledge of TiP preparation is also the direct silica addition into the TiP -syntheses, which is expected to benefit industrial uses of these compounds. Full characterization of both, TiP and TiPSi, and establishing effects of silica on the structure and sorption properties of these materials were the leading paths. The initial material and the effect of silica particles on the TiP matrix are investigated using XRD, TG, BET, IR, SEM, and solid-state NMR techniques. The uptake of cesium and strontium ions by TiPSi at different experimental conditions is studied in detail along with the kinetics of their sorption.

Experimental Section

Synthesis procedure. Solid $TiOSO_4 \cdot H_2O$ (Reahim) was used as a source of titanium. In a typical synthesis procedure, 50 mL aqueous solution of $TiOSO_4$ (containing 1.25 M TiO_2 and 4.8 M H_2SO_4) and the required amount of aqueous Na_2SiO_3 solutions (containing 1 M SiO_2) were combined to satisfy the following molar ratios TiO_2:SiO_2 = 1:0.0−1.0 (mixture A). The obtained mixture is heated up to 60−70 °C for an hour under stirring. Mixture A was combined further with mixture B (4.3 M H_3PO_4 aqueous solution) according to the TiO_2:P_2O_5 = 1 molar ratio and was then allowed to react at 70 °C for 10 h, under stirring. The resulting solid was filtrated, washed consequently with 0.25 M H_3PO_4 (to remove SO_4^{2-} ions) and double-distilled water until pH 3−3.5. The final product (white solids) was dried at 60 °C. For some experiments (see further), the samples were additionally treated with 0.1 M NaOH to convert the H-TiP/TiPSi-form into a salt form (Na-TiP/TiPSi- form). All synthesis procedures and sample handling were performed at laboratory conditions.

The ion-exchange properties of synthesized materials were studied using their granulated forms, whereas all other characterizations were performed on the powder samples.

Sample Characterization. The chemical composition of samples was determined using an ICPE 9000 (SHIMADZU) spectrometer.

Thermogravimetric (TG) and differential thermal analysis (DTA) of the samples were carried out in an argon atmosphere using a high-resolution thermogravimetric analyzer (Model Netzch STA 409/QMS) in a range of 25−900 °C with a heating rate of 10 °C·min^{-1}.

(14) Alberti, G.; Galli, P. C.; Constantino, U.; Torracca, E. *J. Inorg. Nucl. Chem.* **1967**, *29*, 571.
(15) Ahrland, S.; Albertsson, J.; Oskarsson, A.; Niclasson, A. *J. Inorg. Nucl. Chem.* **1970**, *32*, 2069.
(16) Ahrland, S.; Bjork, N.-O.; Blessing, R.; Hermans, R. *J. Inorg. Nucl. Chem.* **1974**, *36*, 2377.
(17) Behrens, E. A.; Clearfield, A. *Microporous Mesoporous Mater.* **1997**, *11*, 65.
(18) Clearfield, A.; Bortun, A. I.; Khainakov, S. A. *Waste Management* **1998**, *18*, 203.
(19) RF Patent 2207980, **2003**.

Powder X-ray diffraction studies of synthesized and calcined (160−750 °C) samples were performed using a Siemens D 5000 diffractometer with a monochromatic Cu K_α radiation ($\lambda = 1.5418$ Å). Scanning rate of 2.4° min^{-1} was used for a 2θ diffraction angle range of 3−50°.

To characterize the surface properties of the titanium phosphates, the BET surface areas and total pore volumes of samples were determined by nitrogen adsorption/desorption method at the liquid nitrogen temperature using a surface area analyzer Micrometrics ASAP 2000. The pore size distributions were determined according to the BJH method (using the desorption branch of the isotherm). Prior to adsorption/desorption measurements, all samples were degassed at 373 K for 4 h. This low degassing temperature was chosen to avoid any structural changes in the materials.

The morphologies of the samples were studied using a Philips XL 30 scanning electron microscope (SEM) equipped with a LaB_6 emission source. A Link ISIS Ge energy dispersive X-ray detector (EDS) attached to the SEM was used to additionally probe the Si distribution within the TiPSi materials.

Infrared (IR) spectra were recorded on a Fourier transform IR spectrometer (PerkinElmer FTIR 2000). A resolution of 4 cm^{-1} was used with 100 scans averaged to obtain a wavenumber spectrum ranging from 4000 to 370 cm^{-1}. The spectra were recorded in IR-grade KBr phase at room temperature.

Solid-state ^{31}P NMR experiments were recorded at 145.71 MHz on a Varian/Chemagnetics InfinityPlus CMX-360 ($B_0 = 8.46$ T) spectrometer. The spectra were acquired using a Varian 4 mm MAS probe and samples were packed in standard ZrO_2 rotors. Ten kHz spinning frequency was used. Spin−echo pulse sequence (5.0 μs - τ_r - 10 μs, $\tau_r = 100$ μs) experiments with proton-decoupling and 1s relaxation delays were used. 256 transients were averaged. All spectra were externally referenced to 85% H_3PO_4.[20] Deconvolutions of the NMR spectra were performed using both Spinsight (a software provided with the spectrometer) and the *DMfit* program.[21] The resonance lines were simulated with a 75% Gaussian/25% Lorenzian ratio that is closed to the previously reported G/L ratio for titanium phosphate systems.[22] All spectra were well fitted with a maximum of three resonance lines.

^{29}Si NMR spectra were recorded at 71.51 MHz on the same spectrometer. A single-pulse experiment with a proton-decoupled acquisition was used. A 6k Hz spinning frequency was used. ^{29}Si 30° pulse width of 1.5 μs and 10 s relaxation delays were used to avoid saturation of signals. About 30000 numbers of acquisitions were averaged. The compounds were additionally studied using ramped cross polarization (CP)[23] from protons and proton decoupling.[24] The CP mixing time was 0.5 ms and ^1H 90° pulse width was 5 μs. About 15 000 transients were averaged with relaxation delays of 5 s. All spectra were externally referenced to TMS, whereas CP-parameters were adjusted using $(CH_3)_3Si(CD_2)_2COONa$ powder.

Amine Intercalation. The intercalation reaction was carried out by liquid−solid method. Prior to the reaction, the sample was dried at 100 °C for 4 h. Twenty milliliters, 0.1 M solution of *n*-propylamine was added to 1 g of titanium phosphate (2 mmol·g^{-1}). The suspension was allowed to react for 5 days at room temperature under stirring. A solid phase was separated, washed with double-distilled water, and dried at 160 °C.

Sorption Studies of Metal Ions. Fifty milliliter, 0.5 g·L^{-1} CsCl (or $SrCl_2$) aqueous solutions with pH 6−6.5 were used in the absorption experiments. About 0.25 g of TiP/TiPSi was added to the solutions, and the resulting suspensions were shaken mechanically for 24 h. (Preliminary data showed that the time required to attain the equilibrium was less than 24 h.) The suspensions were then filtered and pH's of the filtrates were measured. The initial and final concentrations of the metal ion were determined using atomic absorption spectrometer, AAS-300 (PerkinElmer). The results were reproducible within the range of experimental error.

Aqueous solutions of 0.01 M CsCl (or $SrCl_2$) were used to study the sorption properties of TiPSi (0.5 g) at different pH. *V*/*m* were equal to 200. The pH's of the initial solutions were adjusted adding 1 M NaOH or 1 M HCl solutions.

The distribution coefficients, K_d, (in ml·g^{-1}) for Cs^+ and Sr^{2+} in TiPSi at different concentrations of NaCl were determined. K_d was calculated according to the formula,

$$K_d = [(C_0 - C_{eq})/C_{eq}]V/m, \quad (1)$$

where C_0 and C_{eq} are the metal ion concentrations of the initial solutions and of the solutions in equilibria with the exchanger, respectively. *V*/*m* is the volume to mass ratio.

To analyze further the sorption behavior of these cations, sorption isotherms were built. Solutions with different concentration of Cs^+ and Sr^{2+} in 0.05 M NaCl were used. Two hundred milliliters of each solution were allowed to react with 0.5 g silica-modified titanium phosphates for two days. The samples were then analyzed and a dependence of the concentration of Cs^+, and Sr^{2+} in the TiPSi from the equilibrium concentrations of these ions in the solutions was found.

The kinetics of cesium and strontium sorption was studied at 25 °C using the batch method. Solutions of 200 mL, 100 mg·l^{-1} Cs^+ and Sr^{2+} were used. One g TiPSi with 1 mm particle size was used in each case. The sorption was conducted at pH 7−7.5 under stirring (300 rpm). The solutions were kept at 25 °C for 1 h and then the TiPSi-0.03 was added to the systems. During the sorption experiments, concentrations of metal ions in the liquid phase were monitored and the experiments were stopped when the equilibrium concentrations of Cs^+ and Sr^{2+}, respectively, were attained.

To clarify the rate-limiting step of sorption by TiPSi-0.03, the interruption test method was used.[25] The Boyd equation was used to determine whether the rate of ion exchange is governed by diffusion through the sorbent or by diffusion in solution,[26]

$$F = 1 - \frac{6}{\pi^2}\sum_{n=1}^{\infty}(1/n^2)\exp(-n^2Bt) \quad (2)$$

where F denotes the fractional attainment of equilibrium of an exchange process, $D\pi^2/R^2 = B$ is the kinetic coefficient, t is time (s), R is the radius of the ion-exchanger particles (m), D is the diffusion coefficient ($m^2 \cdot s^{-1}$), and n represents natural numbers.

The experimental fractional attainment of equilibrium F, is calculated as $F = X_t/X_\infty$, using the values for the metal uptake (mg·g^{-1}) at time t and the maximum uptake (for X_∞). Tabulated Bt values (corresponding to the solutions of the Boyd equation)[26,27]

(20) Karaghiosoff, K. *Encyclopedia of Nuclear Magnetic Resonance*; Wiley, New Work, 1996; *6*, p 3612.
(21) Massiot, D.; Fayon, F.; Capron, M. et al. *Magn. Reson. Chem.* 2000, *40*, 70. *DMfit* program is available at http://crmht-europe.cnrs-orleans.fr.
(22) Sanz, J.; Iglesias, J. E.; Soria, J. *Chem. Mater.* **1997**, *9*, 996.
(23) Metz, G.; Wu, X. L.; Smith, S. O. *J. Magn. Reson. Ser. A* **1994**, *110*, 219.
(24) Pines, A.; Gibby, M. G.; Waugh, J. S. *J. Chem. Phys.* **1972**, *56*, 1776.
(25) Khraishuh, M. A. M.; Al-Degs, Y. S.; Allen, S. J.; Ahmad, M. N. *Ind. Eng. Chem. Res.* **2002**, *42*, 1651.
(26) Boyd, G. E.; Adamson, A. W.; Myers, L. S. *J. Am. Chem. Soc.* **1947**, *69*, 2836.
(27) Pathak, R. N.; Choppin, J. P. *J. Radioanal. Nucl. Chem.* **2006**, *270*, 299.

Table 1. Chemical Composition and Surface Properties of Initial and Modified Titanium Phosphates

sample	P/Ti (mole)	Si/Ti (mole)	SiO_2 (mole)	H_2O (mole)	SA, $m^2.g^{-1}$	total pore volume, $cm^3 \cdot g^{-1}$	average pore diameter, nm
TiP	1.32	0		2.30	94.4	0.53	20.8
TiPSi-0.01	1.27	0.03	0.015	2.35	96.1	0.51	19.6
TiPSi-0.03	1.24	0.06	0.033	2.40	113.0	0.50	16.2
TiPSi-0.05	1.22	0.10	0.050	2.46	130.0	0.47	13.4
TiPSi-0.08	1.20	0.18	0.078	2.52	148.8	0.45	12.6
TiPSi-0.10	1.18	0.25	0.100	2.59	117.7	0.45	14.1

are used to plot $Bt = f(t)$. Diffusion coefficients were then determined from the slope B and the known radius of the ion-exchanger particles.

Results and Discussion

Characterization of Titanium Phosphate Materials. The elemental data analysis and porous characteristics of silica-free TiP are listed in Table 1. Data show that the obtained TiP solid is characterized with P/Ti molar ratio of 1.32 and relatively high surface area of about 94 $m^2\ g^{-1}$.

The XRD powder patterns of the initial (a) and the calcined at 750 °C (c) titanium phosphates are displayed in Figure 1. The absence of sharp peaks in the X-ray powder diffractograms obtained after calcinations from 60 to 600 °C (not shown) suggests the amorphous nature of the material. A crystalline phase with interlayer distance of 3.7 Å is formed after calcination of TiP at 750 °C. The latter powder pattern

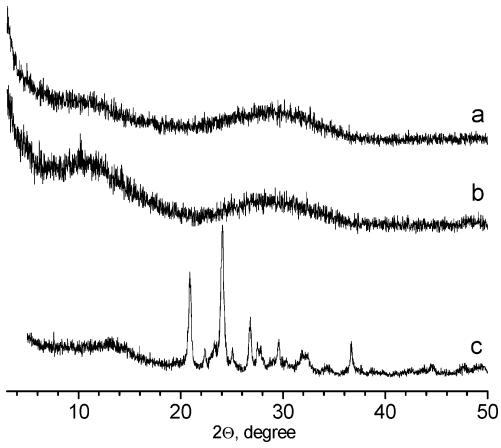

Figure 1. XRD powder patterns for titanium phosphates: (a) initial TiP, (b) *n*-propylamine intercalated TiP, and (c) calcined at 750 °C TiP.

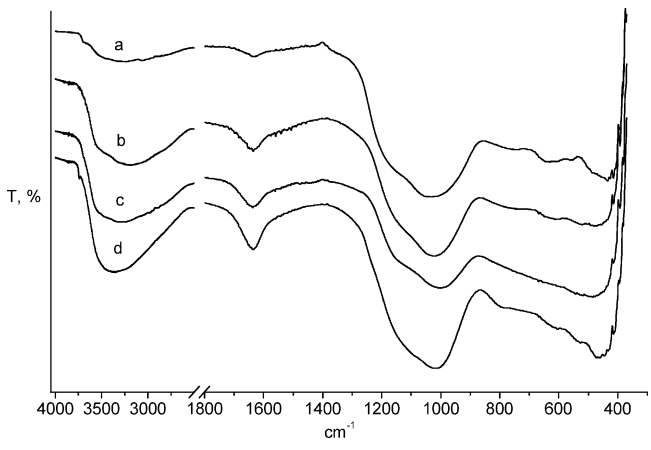

Figure 2. FTIR spectra of titanium phosphates (a) calcined at 400 °C TiP, (b) calcined at 160 °C TiP, (c) *n*-propylamine intercalated and calcined at 160 °C TiP, and (d) TiPSi-0.10 calcined at 160 °C.

was compared to an XRD pattern of titanium polyphosphate, $Ti_4P_6O_{23}$, and the similarity was confirmed. However, the presence of impurities, evident by a few poorly resolved peaks of very low intensity, cannot be excluded. According to the chemical analyses data for P/Ti ratio in Table 1, these peaks could be due to a form of TiO_2.

The IR spectrum of initial TiP calcined at 160 °C is shown in part b of Figure 2 (a similar IR spectrum was obtained for initial TiP dried at 60 °C, not shown). This is a typical spectrum for amorphous titanium phosphates. The broadband around 3400 cm^{-1} is due to overlapping asymmetric and symmetric OH stretching vibrations of present water molecules and P−OH groups. The band at 1635 cm^{-1} is in general referred to the OH bending vibration of adsorbed water. The absorption band at 1035 cm^{-1} is assigned to the Ti−O−P stretching modes of HPO_4^{2-} groups, whereas the band at 436 cm^{-1} is attributed to the P−O bending vibrations.[28,29] In the IR spectrum of TiP, calcined at 400 °C, (part a of Figure 2) the OH^- stretching and bending vibrations of residual water are poor resolved, and the P−O stretching and bending modes are less pronounced most likely due to condensation of the phosphate groups. At the same time the vibration bands at 748 and 630 cm^{-1} became more resolved. The band at 630 cm^{-1} is a characteristic of either Ti−O−P vibrations[13] or of the P−O−P symmetric stretching vibrations (providing that condensation takes place).[30] The frequency of 750 cm^{-1} has been assigned to nonbridging oxygen Ti−O bond vibrations and has been attributed to the presence of terminal OH groups.[31,32] It is likely that at 400 °C the phosphate-condensation process is not fully completed and a part of the OH groups remains bound to the titanium. All of this data strongly indicate that the TiP contains OH groups connected to titanium and that it is a hydroxyphosphate material. Vibrations in the region below 630 cm^{-1} can be explained by out-of-plane P−OH deformation modes.[29]

The ^{31}P MAS NMR spectrum of the initial titanium phosphate calcined at 160 °C is shown in Figure 3. A relatively broad peak (10−40 ppm) is observed due to the amorphous nature of phosphate framework where different phosphorus environments are expected. A deconvolution procedure was applied to determine the chemical shifts of the main P-species present in the initial TiP. The best fit of data was obtained when three-line deconvolution was used

(28) Nilchi, A.; Maragheh, M. G.; Khanchi, A. *J. Radioanal. Nucl. Chem.* **2004**, *261*, 393.
(29) Sahu, B. B.; Parida, K. *J. Colloid Interface Sci.* **2002**, *248*, 221.
(30) Guler, H.; Kurtulus, F. *Mater. Chem. Phys.* **2006**, *99*, 394.
(31) Sakka, S.; Miyaji, F.; Fukumi, K. *J. Non-Cryst. Solids* **1989**, *89*, 64.
(32) Chernokurov, N. G.; Korshunov, I. A.; Zhuk, M. I. *Russ. J. Inorg. Chem.* **1982**, *27*, 1728.

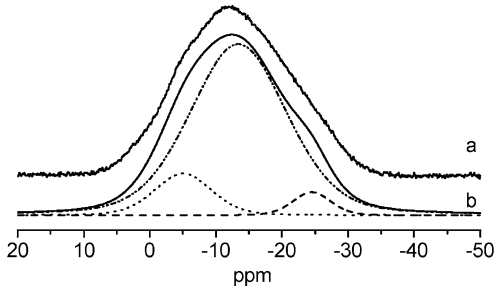

Figure 3. The ^{31}P MAS NMR spectrum of nonmodified titanium phosphate (a) along with simulations using three components (b). The spinning frequency is 10 kHz.

(as shown in part b of Figure 3). It has been reported that a correlation between the connectivity and the chemical shift for phosphorus in titanium phosphates exists. As the connectivity increases, an upfield shift is observed from −5.3 to −10.6 ppm for $H_2PO_4^-$, to −18.1 ppm for HPO_4^{2-}, and finally from −19 to −32.9 ppm for PO_4.[33−36] In another study, a set of amorphous TiP samples with a P/Ti ratio from 0.5 to 2 have been studied using ^{31}P MAS NMR.[13] It is interesting to note that when P/Ti was in the range of 1.25−1.33 (that is similar to the range obtained within this study, Table 1), the ^{31}P NMR spectra obtained were very similar to the spectrum shown here in Figure 3. On the basis of the aforementioned studies, we assign the ^{31}P NMR resonance lines at the chemical shifts of −5.0, −13.4, and −24.3 ppm to the phosphorus sites in $H_2PO_4^-$, HPO_4^{2-}, and PO_4^{3-} environments, respectively, and consider that the HPO_4^{2-} groups are the dominant species. The $H_2PO_4^-$ and PO_4^{3-} species are likely to be formed on the edges of TiP particle surfaces and coexist with the structural-formatting HPO_4^{2-} species.

Sodium forms of the TiP, calcined at 160 and 400 °C, show similarly broad phosphorus resonances that are deconvoluted into three resonance lines with different chemical shifts. It should be noted here that it is practically impossible to prepare completely substituted salt forms of the amorphous titanium phosphates as increasing the alkalinity leads to TiP decomposition.[37] A comparison of the ^{31}P-chemical shifts for hydrogen and sodium forms of TiP shows a downfield chemical shift change that is most likely due to the sodium electronegativity. The interactions with water are expected to result also in a downfield shift,[34] and this can be seen in the slight differences in δ_{iso} (^{31}P) for the sodium forms of TiP calcined at 400 and 160 °C, respectively. All ^{31}P NMR data are summarized in Table 2.

The combination of IR and NMR data reveals the presence of OH^- in the vicinity of the titanium and the presence of dominant HPO_4^{2-} groups. Therefore, we suggest that the most likely chemical formula of TiP is $Ti(OH)_{2x}(HPO_4)_{2-x}\cdot nH_2O$, where the HPO_4^{2-} are the main ion exchanging groups.

Table 2. ^{31}P Isotropic Chemical Shift Data for Titanium Phosphates Obtained at Different Conditions

syntheses conditions for TiP	δ_{iso} (ppm)
160 °C, hydrogen form	−5.0, −13.4, −24.3
160 °C, sodium form	−0.1, −6.1, −12.2
400 °C, sodium form	−0.2, −7.9, −16.8
160 °C sodium form (amine intercalated)	2.2, −2.3, −7.4

Furthermore, adsorption of *n*-propylamine from liquid phase was undertaken to probe the structure of initial TiP. The XRD powder pattern of amine-intercalated titanium phosphate (part b of Figure 1) shows a slight difference in the range of $2\theta = 8-12°$, which indicates that the synthesized material was indeed reacting with the amine. The IR spectrum of TiP intercalated with *n*-propylamine and calcined at 160 °C (part c of Figure 2) shows some differences from the IR spectrum of initial TiP. The band due to phosphate stretching modes (1035 cm^{-1}) decreases its intensity, whereas intensity of the P−O bending vibration mode increases. These changes in the phosphorus arrangement imply that the phosphorus groups in TiP became more protonated. More pronounced differences were indeed observed in the ^{31}P MAS NMR spectra of these systems. A comparison of the $\delta_{iso}(^{31}P)$ for initial TiP and for *n*-propylamine intercalated TiP samples (both sodium forms, calcined at 160 °C) shows a considerable downfield shift that is most likely due to insertion of the amine into the TiP framework. Similar differences in the $\delta_{iso}(^{31}P)$ have been observed for $Zr(HPO_4)_2\cdot H_2O$ and its *n*-propylamine intercalated form and were associated with the properties of the layer-like Zr-hydroxyphosphate structure.[38] Analogously, it can be said that the TiP synthesized in this work possesses a layer-like structure.

To obtain further information about structural features of TiP, a TG analysis on the initial sample was performed. The TGA data (part a of Figure 4) show that a thermal decomposition of TiP takes place in the temperature range of 100−900 °C, and the final product is a mixture of $Ti_4P_6O_{23}$ and a negligible amount of TiO_2 as confirmed by powder XRD. According to TG-DTA data, the first DTA peak at 100 °C is due to a release of physically adsorbed water (weight loss of 7.3%). When all of the water is liberated, Ti-OH and HPO_4^{2-} groups start to condense. These processes take place simultaneously in the temperature ranges of 160−260 °C (8.1% weight loss) and of 260−700 °C (2.3% weight loss) respectively and result in an overlap of the TG data. The total weight loss up to 700 °C is 17.7%, and no further mass loss is observed. The DTA curve shows two exothermic peaks at 700 and 835 °C that corresponds to a two-step exothermic transformation of TiP into a polyphosphate phase.

The nitrogen adsorption−desorption measurements were utilized to study the porous characteristics of the titanium phosphates. Part a of Figure 5 shows the N_2 adsorption−desorption isotherm (at 77 K) for the initial TiP sample. The isotherm can be categorized as type IV according to the Brunauer classification and is typical for mesoporous materials. According to the IUPAC classification, which defines the different types of hysteresis loops, the observed loop can

(33) Takahashi, H.; Oi, T.; Hosoe, M. *J. Mater. Chem.* **2002**, *12*, 2513.
(34) Bortun, A. I.; Bortun, L. N.; Clearfield, A. *Solv. Extr. Ion. Exch.* **1996**, *14*, 341.
(35) Li, Y. J.; Whittingham, M. S. *Solid State Ionics* **1993**, *63*, 391.
(36) Jones, D. J.; Aptel, G.; Brandhorst, M.; Jacquin, M. *Chem. Mater.* **2000**, *10*, 1957.
(37) Bortun, A. I.; Khryashevskii, V. N.; Kvashenko, A. *Ukr. Khim. Zh.* **1991**, *57*, 806.
(38) MacLachlan, D. J.; Morgan, K. R. *J. Phys. Chem.* **1992**, *96*, 3458.

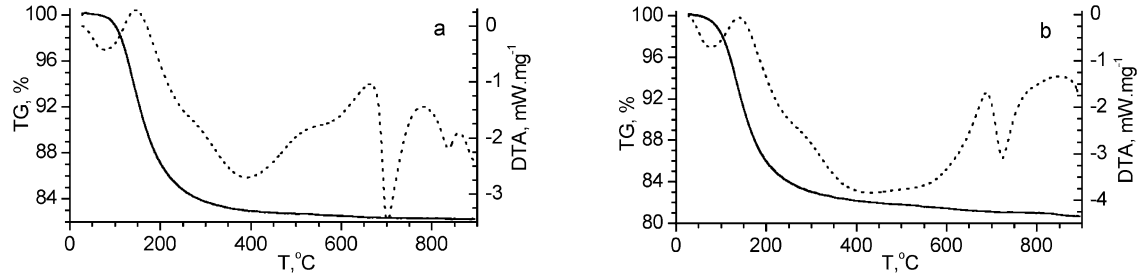

Figure 4. TG (solid line) and DTA (dashed line) curves for TiP (a) and TiPSi-0.10 (b).

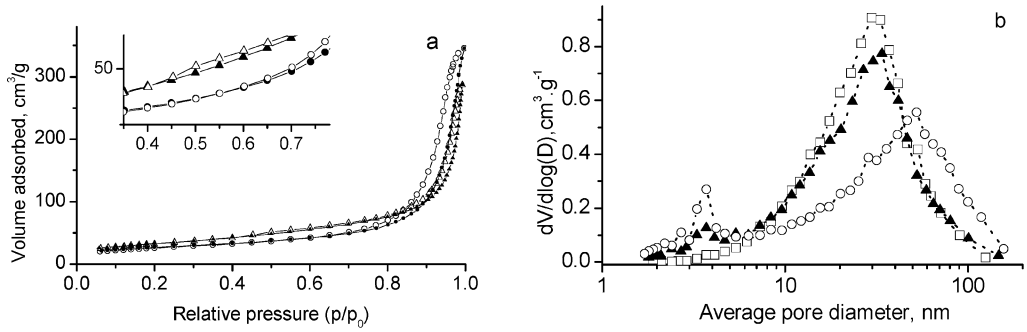

Figure 5. Nitrogen adsorption isotherms (a) of TiP (•) and TiPSi-0.10 (▲), solid/open symbols corresponds to adsorption/desorption, respectively; (b) BJH pore size distribution plots of TiP (□), TiPSi-0.03 (▲), and TiPSi-0.10 (○).

be considered as H1 type that is often obtained for samples consisting of agglomerated spherical particles of fairly uniform size.[39] This hysteresis loop in the high relative pressure region ($p/p_0 > 0.65$) is related to the capillary condensation associated with the presence of larger pore cavities, suggesting sizes mainly in the mesopore range. The pore size distribution calculated on the basis of BJH analysis (from the desorption branch of the isotherm) is rather broad with a maximum at about 30 nm (part b of Figure 5).

Cross analyses of all data for TiP obtained in this study confirm that the initial sample is a mesoporous layered titanium hydroxyphosphate with formula $Ti(OH)_{1.36}(HPO_4)_{1.32}$ $2.3H_2O$.

Characterization of Silica-Modified Titanium Phosphate Materials. The elemental analyses data for compositions of the silica-modified titanium phosphates-TiPSi are listed in Table 1. It can be seen that with an increase of silica amount the P/Ti ratio decreases, which on the one hand is expected to govern a lower number of functional phosphate groups in the final products. The increase of silica amount also leads to an increase of the water content. The specific surface area (SA) of TiPSi materials increases from 94 m^2g^{-1} (for TiP) to 149 m^2g^{-1} (TiPSi-0.08) with an increase of silica content. The last sample is an exception of this trend and shows a SA of 117 m^2g^{-1}. This fact might be explained with formation of a denser silica modification in the sample with the highest silicon content within the series. In the following discussion, the TiPSi-0.0*X*, *X* refers to the measured amount of SiO_2 (mole).

Figure 6 shows a plot of amount of SiO_2/TiO_2 used in the syntheses versus the amount measured in the samples. The lower amount of silicon found in the TiPSi samples relative to the nominal amounts used in the synthesis can be explained by the fact that precipitated amorphous silica is expected to partly redissolve during the postsynthesis washing with ortho-phosphoric acid.

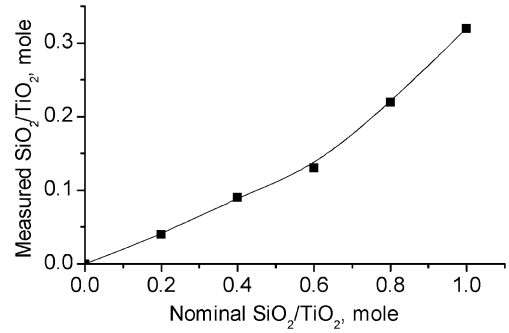

Figure 6. SiO_2/TiO_2 ratio in TiPSi versus the nominal synthesis ratio. The line is a guide for the eye.

During the synthesis of silica-modified titanium phosphates, two main processes can occur: (i) silica can incorporate into the TiP framework and/or (ii) it can coprecipitate as an independent phase. These processes would be expected to cause functionalization of the material surface and formation of new sites. Toward revealing the origin of silica in the modified titanium phosphates the IR, NMR, DTA, BET, and SEM data of these systems were analyzed.

Part d of Figure 2 shows the IR spectra of modified sample with highest SiO_2 content (0.10 mol). The vibration modes observed do not differ significantly from the bands observed in the IR spectrum of nonmodified TiP. The intensity of OH stretching vibration mode at around 3500 cm^{-1} is somewhat increased and this is likely to be caused by hydration of silica sites. The absorption bands due to the −Si−O−Si− and Si−OH vibrations in the 960−1100 cm^{-1} region[40,41] are overlapped with the strong Ti−O−P stretching vibration. The band at 800 cm^{-1} is assigned to the vibration of Si−OH groups, and it is only seen in this sample (TiPSi-0.10). The

(39) Gregg, S. J.; Sing, K. S. W. *Adsoption, Surface Area and Porosity*, 2nd ed.; London, 1982.

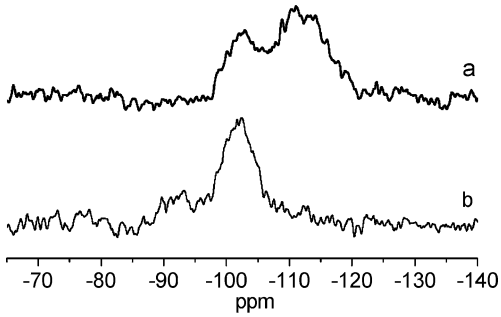

Figure 7. ^{29}Si MAS NMR spectra of TiPSi-0.10: (a) 1-pulse experiment, (b) ^{1}H−^{29}Si cross polarization experiment. The spinning frequency is 6 kHz.

band at 785 cm^{-1} that characterizes the titanium silicates[42] is not detected here. Therefore, it can be proposed that silica in TiPSi is mostly in a Si−O−Si environment and that a titanium silicate phase is not formed in these samples. Silica is likely coprecipitated in the TiP matrix in a uniform manner without forming a new compound.

Silica-modified TiP samples neither show major changes in the XRD powder patterns nor in the ^{31}P NMR spectra compared to the initial titanium phosphate, which suggest further that new compounds were not formed at these conditions.

The ^{29}Si NMR spectra of the sample with highest amount of silica (TiPSi-0.10) obtained at two different experiments are shown in Figure 7. The presence of two broad silicon resonances centered at −101.6 and −111.4 ppm respectively is observed in the single-pulse experiment. The cross-polarization from protons experiment performed on the same sample results in recording only silicon sites at −101.6 ppm (and a considerably weaker signal at −92 ppm). The absence of the resonance at −111.4 ppm in the CP/MAS experiment shows that there are no hydrogen atoms in a close vicinity to these silicon sites. These data confirm that the silicon species with isotropic chemical shift at −111.4 ppm belong to the classic Q^4 Si type (4Si, 0Ti) that is a characteristic of fully polymerized silica species.[43] It has also been reported that silica fume exhibits a broad ^{29}Si NMR resonance at −111.5 ppm,[44] and therefore it can be suggested here that a part of silica in the titanium phosphate matrix is in a similar oxygen environment. The species at −101.6 and −92 ppm are of the corresponding Q^3 and Q^2 types most likely related to the presence of silanol groups on the surface of particles.[43]

The thermal analysis of TiPSi-0.10 (part b of Figure 4) shows a gradual weight loss with a total amount of 19.4% up to 900 °C that is 1.7% more than for the silica-free TiP. The first DTA peak is observed at 100 °C with a weight loss of 8.4% that is slightly higher than the weight loss detected for the nonmodified TiP. The processes of condensation of hydroxyl and phosphate groups take place in the similar temperature ranges with weight losses of 7.9% and 2.6% respectively, which are close to the values for the initial TiP. One exothermic peak due to transformation of phosphate to polyphosphate species is observed at 725 °C, and this is likely to be related to the presence of silica.

The increase of amount liberated water can be correlated to the larger surface area of the samples (Table 1). The latter is somewhat governed by silica presence, which is naturally characterized with a relatively high surface area and porosity. In turn, this is expected to lead to a higher content of adsorbed water and this is indeed confirmed with the IR spectra of TiPSi.

Part a of Figure 5 shows the adsorption−desorption isotherm of silica modified TiP. It belongs to the aforementioned type IV that is characterized with a sloping adsorption branch and a steep desorption branch. The hysteresis loop is a combination of H1 and H3 types (p/p_o = 0.4−0.6) indicating presence of platelike particles.[39] The hysteresis closure point in the isotherm is observed at a lower relative pressure (inset), and this is attributed to presence of pores in the range of wide micropores and/or narrow mesopores. The latter is more clearly visible in the pore size distribution plot, as seen in part b of Figure 5. The pore size distribution curves for TiP and TiPSi show that SiO_2 modification leads to a shift of the distribution maximum to a higher value and that a new relatively well-defined maximum corresponding to pore size of about 4 nm is formed. It has been reported that very close to 4 nm a maximum related to the tensile strength effect (TSE) appears.[45] To avoid misinterpretations, a similar plot was built using the adsorption branch of the isotherm (not shown), and no formation of a new maximum with increasing the silica content in the samples was observed. Therefore, the peak at 4 nm shall be considered as an artifact due to the TSE. The shift of the maximum in the pore diameter distribution for TiPSi samples toward wider pores suggests that the increased amount of silicon results in filling in the narrow mesopores. This is in a very good correlation with the facts that both the average pore diameter and the total pore volume of TiPSi materials decrease as the SA increases (Table 1).

All of this data show that silica in the modified TiP affects mainly the interparticle porous system of these materials, and the major changes are relevant to pores in the mesoporous range.

The morphology of the initial and silica-modified TiP products was characterized by scanning electron microscopy (SEM). All materials show a similar morphology of relatively small amorphous particles with an average size of 100 nm and irregular shapes. SEM images of initial TiP and TiPSi-0.10 are shown in Figure 8. Differences in the particle habits of these materials are clearly seen, revealing presence of different size agglomerates with tunnel-like structures. EDS mapping analyses could not distinguish silica-only islands (even for the sample with highest content of silica in this study), which confirm that silica is evenly distributed in the TiP matrix. All of this leans toward the fact that silica is

(40) Hair, M. *Infrared Spectroscopy in Surface Chemistry*, M. Dekker Inc.: New York, 1967.
(41) Astorino, E.; Peri, J. B.; Willey, R. J.; Busca, G. *J. Catal.* **1995**, *157*, 482.
(42) Alba, M. A.; Luan, Z.; Klinowski, J. *J. Phys. Chem.* **1996**, *100*, 2178.
(43) Mackenzie, K. J. D.; Smith, M. E. *Multinuclear Solid-State NMR of Inorganic Materials*; Pergamon: Amsterdam, 2002.
(44) Rowles, M. R.; Hanna, J. V.; Pike, K. J.; Smith, M. E.; O′Connor, B. H. *Appl. Magn. Reson.* **2007**, *32*, 663.
(45) Groen, J. C.; Peffer, L. A. A.; Perez-Ramirez, J. *Microporous Mesoporous Mater.* **2002**, *51*, 75.

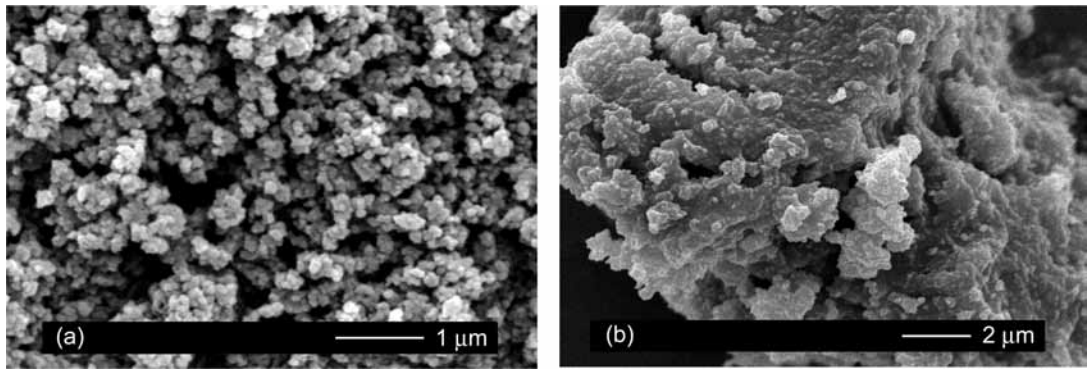

Figure 8. SEM images of initial TiP (a) and TiPSi-0.10 (b).

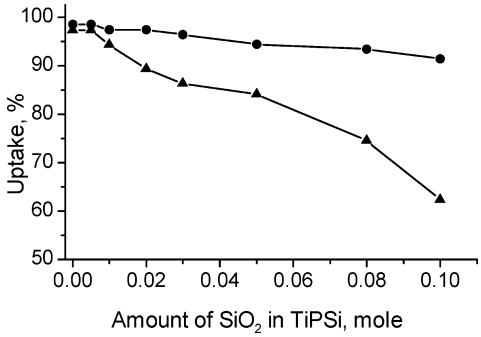

Figure 9. Cs^+ (•) and Sr^{2+} (▲) uptake by silica-modified titanium phosphates at pH 6.5. The lines are a guide for the eye.

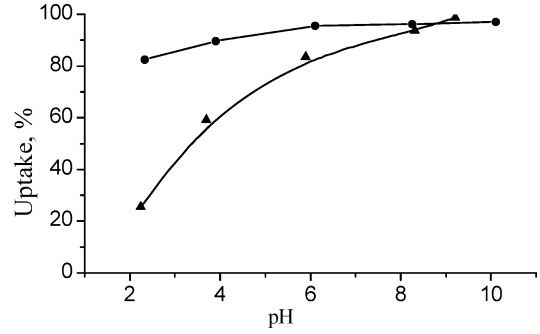

Figure 10. Cs^+ (•) and Sr^{2+} (▲) uptake by TiPSi-0.03 at different pH. The lines are a guide for the eye.

coprecipitated in the TiP matrix and that it is unlikely to have a concomitant incorporation process.

All spectroscopic data together with the BET and SEM analyses show that the composition of TiPSi can be expressed as $Ti(OH)_{2x}(HPO_4)_{2-x}\cdot ySiO_2\cdot nH_2O$, and the main ion exchange sites of these materials are expected to be HPO_4^{2-}.

Ion-Exchange Properties of Silica-Modified Titanium Phosphates. As shown in the previous section, the presence of silica considerably alters the pore structure of silica-modified titanium phosphates. Thus, it is reasonable to suggest that the sorption affinity of these materials toward cations with different sizes might be affected. In this study, we choose to compare the uptake for two cations with significantly different sizes − Cs^+ and Sr^{2+}. Their isotopes, ^{90}Sr and ^{137}Cs respectively, are among the radioactive remedies that most often need to be removed to convert the high-level waste into a low-level waste.[17] The data shown in Figure 9 reveal that the Cs^+ uptake (%) is fairly independent of the SiO_2 content in the samples, whereas the Sr^{2+} uptake drastically decreases as the silica amount increases. This behavior is most likely due to the smaller ionic hydration shell of Cs^+ (3.29 Å),[46] which somewhat favors the sorption of these ions, whereas the larger Sr^{2+} hydration shell (4.12 Å)[46] restricts the diffusion processes throughout the TiPSi matrix. Furthermore, this means that functional groups in TiPSi materials with different exposure are responsible for the difference in the cesium and strontium uptakes, that is, most of the ion-exchange sites are available to Cs^+ and only surface sites are accessible for the Sr^{2+}. All of this data leads to the conclusion that the increase of SiO_2 amount in TiPSi affects only the uptake of cations with relatively large hydration shells, and it appears that the diffusion across the TiPSi framework might be playing major role in the ion exchange processes.

All of the following data are obtained on the TiPSi-0.03 sample as the preliminary tests showed that this sample is mechanically resistant and has good ion-exchange properties. The ion exchange affinity of the material toward Cs^+ and Sr^{2+} cations was probed in a wide pH region using the batch technique. The experimental curves showing the cations uptake at different pH values are given in Figure 10. It can be seen that the Cs^+ uptake is almost constant in the studied pH range, whereas the Sr^{2+} uptake increases rapidly with an increase of pH. The data for Cs^+ clearly show that at this wide range of pH values the smaller hydration shell allows the metal cation to unobstructedly penetrate the exchanger in depth. At low pH, the uptake of cesium ions is 82% or 1.65 meq·g^{-1}, and it increases to 97% or 1.94 meq·g^{-1} in a basic medium (pH 8−10).

The data for strontium ions show that the Sr^{2+} uptake rises from 1.00 meq·g^{-1} in an acidic medium to 3.96 meq·g^{-1} in a basic medium (pH 9). With an increase of pH, the deprotonation of hydroxyphosphate groups increases and hence the ion exchange capacity of the TiPSi. It also means that both surface and interlayer active sites become more accessible for the larger ions, and thus the uptake of Sr^{2+} is favored. It has been reported that at pH ≤ 10, 96% of Sr^{2+} remain in solution;[31] therefore, we can assume that at pH 9 a negligible amount of strontium hydroxide precipitate is formed on the TiPSi surface. However, formation of $SrCO_3$ cannot be excluded and this would contribute to the increase of strontium uptake.

(46) Nightingale, E. R., Jr. *J. Phys. Chem.* **1959**, *63*, 1381.

Table 3. Distribution Coefficients of Cs^+ and Sr^{2+} at Different NaCl Concentrations

NaCl, M	K_d, ml·g^{-1}	
	Cs^+	Sr^{2+}
	88 466	66 723
0.05	16 589	27 851
0.10	6133	6083
0.25	2003	1056
0.50	1067	250
0.75	606	109
1.00	465	62
2.00	235	35

To study properties of TiPSi in high ionic strength conditions, sorption experiments using 0.01 M Cs^+/Sr^{2+} solutions in 0.05 −2 M NaCl with solid/liquid phase ratio 1:200 (g:ml) were performed. The experimental data (given in Table 3) show that an increase of electrolyte concentration leads to a decrease of distribution coefficient, K_d for both cations. When 0.05 M NaCl is used K_d of Cs^{2+} is in the range of 10^4 to 10^3 and it decreases more than 100 times when 1−2 M NaCl is used. This trend is even more pronounced for Sr^{2+} where K_d falls to 35 mL·g^{-1}. In concentrated electrolyte solutions (where desolvatation takes place), the selectivity of TiPSi toward Cs^+ is considerably higher (in comparison to Sr^{2+}) due to the smaller hydration shell. Another possibility to be considered is that at a high electrolyte concentration the proton-exchange sites are somewhat closed by Na^+ ions, and this makes it difficult for Cs^+ to diffuse across the TiP framework. The K_d data for the Sr^{2+} show that it is almost impossible for these large ions to penetrate the modified titanium phosphate materials at this high electrolyte concentration. This data strongly indicate that the sorption processes are based on an ion-exchange mechanism.

To analyze further the sorption behavior of these cations, sorption isotherms were built. Figure 11 shows that in both cases the cation uptake rapidly increases at low equilibrium

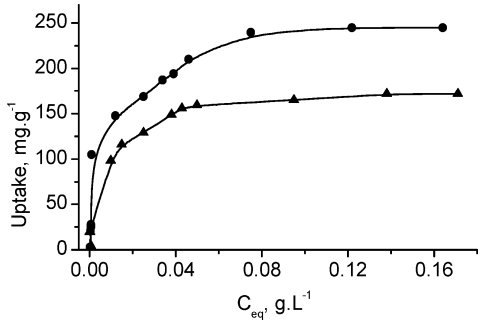

Figure 11. Sorption isotherms of TiPSi-0.03 in the presence of Cs^+ (•) and Sr^{2+} (▲). The lines are a guide for the eye.

Table 4. Kinetic Data for Cs^+ and Sr^{2+} (R = 1 mm)

	Cs^+				Sr^{2+}			
t, min	Xt, mg·g^{-1}	F	Bt^{26}	D·10^{-7} cm^2·s^{-1}	Xt, mg·g^{-1}	F	Bt^{26}	D·10^{-7} cm^2·s^{-1}
5	22.5	0.225	0.06	2.53	15.3	0.15	0.03	1.01
10	35.4	0.35	0.14	2.53	22.8	0.23	0.06	1.02
15	43.2	0.43	0.23	2.31	29.4	0.29	0.09	1.01
20	51.0	0.51	0.32	2.53	32.1	0.32	0.12	1.01
30	60.7	0.61	0.52	2.53	40.4	0.40	0.18	1.01
40	70.3	0.70	0.72	2.95	45.2	0.45	0.24	1.01

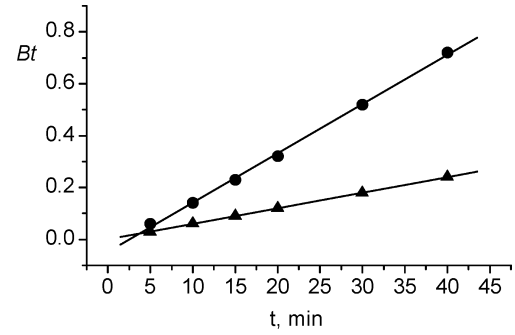

Figure 12. Ion exchange kinetics data along with the corresponding linear fits for Cs^+ (•) and Sr^{2+} (▲) ions.

concentrations of cations and reaches a plateau at about 0.07 g·l^{-1}. The latter allows the ion-exchange capacity of TiPSi-0.03 at these conditions to be calculated. The metal uptake (not shown) increases with an increase of initial concentration of cations up to 400 mg·l^{-1} and then remains constant due to either hindered diffusion and/or the Coulomb repulsion. The uptake for both ions is completed (100%) for solutions with concentrations up to 200 mg·l^{-1}. These data show that the silica-modified titanium phosphates have good sorption properties toward Cs^+ and Sr^{2+} ions.

It is known that kinetics of ion-exchange reactions depend on the rates of following processes: (i) ion-diffusion into solution, (ii) ion-diffusion into the particles (gel-diffusion), (iii) ion-exchange, (iv) counterion diffusion into the particles, and (v) counterion diffusion into solution. The rate-determining step is the slowest process among these processes. Determination of the limiting step is important not only for clarifying the mechanism of ion exchange reaction but also for practical optimization of the ion-exchange process. The limiting step of Cs^+ and Sr^{2+} ion exchange by TiPSi-0.03 was determined using the interruption test method.[25] It was observed that after the interruption period the rate of metal uptake increases for both cations. These data show that the rate of sorption depends on the rate of ion diffusion into the particles process, that is, the gel diffusion is the rate determining step in the ion-exchange process. This was also confirmed when the kinetic data shown in Table 4 and Figure 12 were analyzed. The presence of a straight line in the (Bt, t)-plot supports the fact that the ion-exchange processes in TiPSi have a gel diffusion nature.[26,27] The mean diffusion coefficients obtained for Cs^+ and Sr^{2+} are 2.56·10^{-7} and 1.01·10^{-7} cm^2·s^{-1}, respectively. Half-exchange times ($t_{1/2}$ = 0.03R^2/D) for cesium and strontium ions are 19.5 and 50 min, respectively. These data are in a good agreement with the data reported by Amphlett for similar ion-exchanger systems.[47]

Conclusions

Amorphous titanium hydroxyphosphate, TiP, with formula $Ti(OH)_{1.36}(HPO_4)_{1.32}$ $2.3H_2O$ and a new silica-modified titanium hydroxyphosphate, TiPSi, were synthesized and extensively characterized using a combination of analytical and spectroscopic methods. On the basis of IR, TG, XRD,

(47) Amphlett, C. B. *Inorganic Ion Exchangers*; Elsevier, Amsterdam, 1964.

solid-state NMR, and BET data, the TiPSi composition was determined as $Ti(OH)_{2x}(HPO_4)_{2-x}\cdot ySiO\cdot nH_2O$. Analyses of the data confirmed that SiO_2 was uniformly dispersed in the TiP matrix, and no titanium silicates were formed. The presence of SiO_2 in TiP strongly influenced the textural and sorption properties of the material − with an increase of silica amount the specific surface area of TiPSi increased from about 100 to ca. 150 $m^2\cdot g^{-1}$, whereas both the total pore volume and the average pore diameter decreased from 0.53 to 0.45 $cm^3\cdot g^{-1}$ and from 21 to 14 nm, respectively. The silica-modified titanium phosphates were characterized as mesoporous materials with dominant wide mesopores.

The sorption behavior of TiPSi toward Cs^+ and Sr^{2+} was examined. The sorption of Cs^+ (ca. 95% uptake) did not practically depend on the presence of SiO_2, whereas the Sr^{2+} uptake drastically decreased with an increase of the silica amount, reaching only 60% for the sample with highest silica content. The Cs^+ uptake appeared to be fairly independent of the pH (2−10), whereas Sr^{2+} uptake varied from about 20 to ca. 90% in the same pH region. The ion-diffusion nature of the exchange processes was proven, and the corresponding mean diffusion coefficients for cesium and strontium ions calculated as 2.56×10^{-7} and 1.01×10^{-7} $cm^2\cdot s^{-1}$, respectively.

TiPSi material possesses good sorption and kinetics characteristics with respect to cesium and strontium cations, and it is expected to be suitable for purification of technological solutions and nuclear waste.

Acknowledgment. M. Maslova thanks The Swedish Institute for the financial support of this work. Authors would like to thank Lic. Eng. Ryan Robinson for the TG measurements. The foundation to the memory of J. C. and Seth. M. Kempe is acknowledged for grants (JCK-2003, JCK-2007) used for updating Varian/Chemagnetics CMX-360 NMR spectrometer.

IC801274Z